Description of the Mars Global Cave Candidate Catalog (MGC^3) PDS Archive

G.E. Cushing and C.H. Okubo
USGS Astrogeology Science Center
Flagstaff AZ, 86001

Version 1.0, September 22, 2016

1. Dataset Overview

Simple, basic list of candidates

The Mars Global Cave Candidate Catalog (MGC^3) dataset contains a list of candidate cave-entrance locations on Mars. Most entries in this catalog were identified by surveying images from the Mars Reconnaissance Orbiter's (MRO) Context Camera (CTX) and High Resolution Imaging Science Experiment (HiRISE) cameras. CTX images shows the Martian surface in visible (red) wavelengths at a scale of ~6 m/pixel (*Malin et al.*, 2007), which is sufficient to identify sky-facing, shadowed cave entrance candidates as small as ~25 m across. Many of the highest-quality candidates identified in the CTX survey were subsequently targeted HiRISE, which also observes at visible (red) wavelengths, but at scales as fine as ~0.25 m/pixel (*McEwen et al*., 2007) – or ~1/5000 of a single CTX pixel. This ultrafine resolution achieved by HiRISE is useful to determine which candidates identified in CTX images show evidence that subsurface cavities may extend beyond the observed line of sight (e.g., overhanging rims, surface skylights, etc.); this resolution also provides sufficient detail to characterize fine-scale surface features in and around the caves such as aeolian bedforms, cliff-wall strata and dust/bedrock interfaces. This dataset is being archived with the Planetary Data System (PDS) for use in future planetary cave research. Future contributions of new candidate entrances, the addition of thumbnail images, and refinements to existing measurements will drive subsequent versions of this dataset.

NOTE: Because the candidates listed here have only been observed from Mars orbit, NONE can be verified as genuine caves with cavities extending into dark zones beneath the surface—such verification is not possible until they are physically visited. Historically, the larger portion of candidates identified in CTX images have proven to be false positives (see **Targeting Priority**, below), revealed by HiRISE to be simple pits, depressions, or hard shadows instead of viable cave-entrance candidates.

This archive uses PDS4 archiving standards. An overview of PDS4 is provided in the PDS4 Concepts document (*PDS4 Concepts*, 2015) and the standards are specified in the PDS4 Standards Reference (*PDS4 Standards Reference*, 2015).

2. Data Collection: Cave-entrance survey

The majority of candidates listed here were identified in a survey of CTX images covering Mars' large volcanic regions. These surveys were conducted as part of a project funded by the National Aeronautics and Space Administration's Mars Data Analysis Program (NNH13AV72I) to identify Atypical Pit Crater (APC) locations and compare their erosional states with age estimates for the surrounding terrain. At this time, APCs are only identified in the Tharsis and Elysium regions while other candidate types tend to be more widespread. Survey regions include: Alba Patera, Appolinaris Patera, Cyane Fossae, Daedalia Planum, Elysium Mons, Hadriaca Patera, Nili Patera, Syria Planum, Syrtis Major Planum, Tharsis Montes and Tyrrhena Patera. Viable candidates have not yet been identified in some of these regions. Candidates located outside these primary survey regions were identified either in smaller test surveys or were provided by outside contributors. At this time, the vast majority of Mars has not been surveyed for cave entrances.

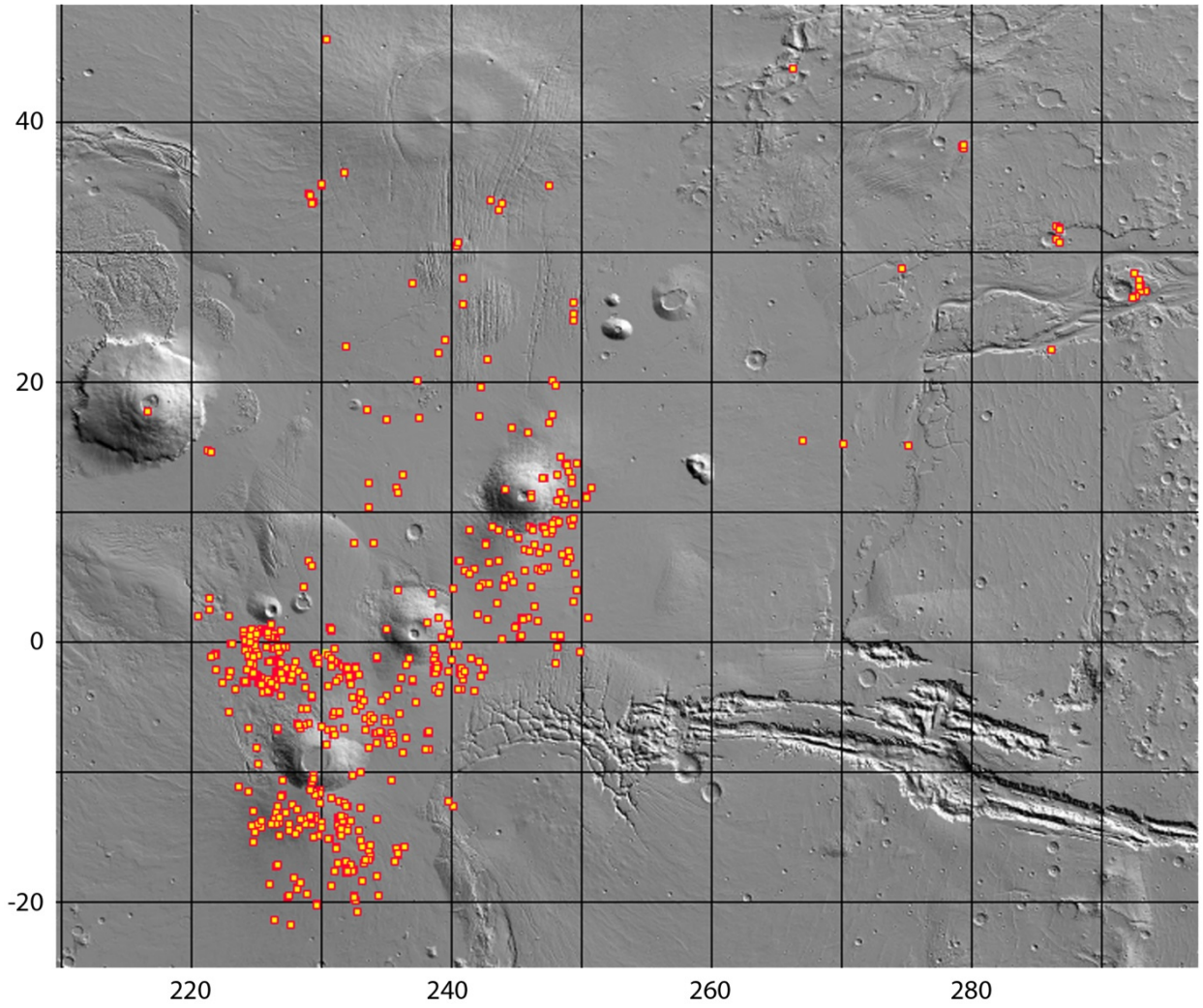


Figure 1. Greatest concentration of recorded cave-entrance candidates. This map includes candidates in: Tharsis Montes, Olympus Mons, Alba Mons, Kasei Valles, Tempe Terra and Daedalia Planum.

We used the Java Mission-planning and Analysis for Remote Sensing (JMARS) planetary GIS tool (*Christensen et al*., 2009) to hand-select a set of CTX image footprints completely covering each region while avoiding excessive image overlaps. Each set of CTX images was downloaded from the PDS archive in raw (.img) format and processed using the U. S. Geological Survey's Integrated Software for Images and Spectrometers (ISIS) cartography software (*Torson and Becker*, 1997; *Gaddis et al*., 2007). Images were processed to jpeg2000 format at native resolution with no map projection. Once processed, each jpeg2000 image was closely scanned at 1:1 magnification (at ~6 m/pixel) using the HiView image viewer (free download at http://www.uahirise.org/hiview/). Candidate entrances were verified and evaluated in all available images covering each scene, then recorded as a point in a JMARS shape layer. JMARS was used to identify footprints and record shape-file points, but was not used to conduct the image surveys because it is a web-based tool that cannot accommodate rapid panning through high-resolution imagery.

Candidate selection criteria: Selection is subjective, and each individual evaluation is based upon numerous factors including: observed solar incidence angle, emission angle, atmospheric haze, sharpness of shadow edges, comparative darkness between candidate shadow and other shadows in scene, morphologies of adjacent terrain features, apparent local aeolian activity, local dust mantling, and differences in overlapping imagery. Each candidate is assigned a 'Targeting Priority' rating based on subjective evaluations, using the above criteria, of the likelihood a candidate will exhibit cave-like characteristics when observed at scales of ~0.25-0.5 m/pix (see 'Targeting priority,' below). False-positive candidates are common, and nearly 25% of the highest-priority candidates observed by HiRISE thus far have turned out to be steep-walled pits, deep shadows or open alcoves without indication of void spaces extending beneath the surface.

3. Data Product Structure

The primary PDS4 product for MGC^3 consists of two files: the PDS4 label and the data table. The PDS4 label (*.xml) is a XML file that contains metadata about how the data in the table were acquired and information on the physical structure of the table. The data table contains 8 columns of information, described below.

Data Table Column Descriptions

The table currently contains 1036 rows of data. Each row describes a single candidate and has 8 columns with a combined total of 110-characters.

Columns:

C-1. ID (Characters 1-6) - There are 2 groups of features in the data table: Atypical Pit Craters (APCs) and Cave entrance candidates. All IDs are 6 characters in length. APCs are identified as

'APC###' and Cave-entrance Candidates are labeled as 'CC####'. Candidates are not arranged in any particular order, although adjacent candidates are often listed in sequential order.

C-2. Longitude (Characters 8-16) – [0-360] Eastward-positive in decimal degrees.

C-3. Latitude (Characters 18-26) – [+/- 90] Planetocentric values in decimal degrees. Southern locations are denoted by negative values.

C-4. Type Code (Characters 28-30) - To aid with sorting candidates according to morphological distinctions we have loosely associated each with a 3-letter code corresponding to visible appearance. Note – codes may be adjusted in subsequent releases of this catalog, as new details in future observations.

Candidate type codes:

APC – Atypical Pit Crater [*Cushing*, 2012; *Cushing et al*., 2015]. Some terrestrial analogs to these structures contain cave entrances (*Okubo and Martel*, 1998; *Cushing et al*., 2015).
crk – Candidate in the form of a deep, dark crack or fracture.
end – Candidate located at the distal end of a channel, fracture or trough.
flr – Candidate is located in the floor of a channel, fracture or trough.
irr – Candidate has an irregular shape and/or other categories are not suitable.
kst – Candidate formed in karst-type terrain (e.g., periglacial or thermokarst terrains)
lat – Candidate has a lateral entrance, often located in cliff walls.
pin – Candidate is a small, sharply defined hole or pit only a few pixels across (pinhole).
pit – a generic, amorphous collapse pit – smaller than APCs and non-circular.
pol – candidate located in polar ice region
rim – Candidate (or cluster of candidates) located on the rim of a pit, channel or trough.
sky – Skylight entrance into a lava tube.
srp – Candidate is a small, shallow and circular rimless collapse pit.

C-5. Targeting Priority (Character 32) – This is an entirely subjective evaluation denoting either 1) the likelihood that high-resolution targeting will reveal a cave or cave-like void extending out of sight beneath the surface; or 2) how 'important' the candidate may be in terms of a specific characteristic such as an important location, underrepresented type, etc.. a '1' represents the highest targeting priority (at the time of this release, ~25% of the highest rated candidates observed by HiRISE did not exhibit cave-like features such as laterally extending voids). Features with a '1' rating are either A) APCs, which are all targeted for an ongoing study of thermophysical characteristics (see *Cushing et al*., 2015); B) features that show unambiguous void spaces or overhangs in CTX imagery; or C) features representing under-sampled candidate types (see Type

Code, above). A rating of '2' signifies a candidate that appears visibly consistent with a cave entrance in CTX imagery, but will most likely not be a cave when viewed at high resolution. The '3' rating represents cave-like features of interest but are sufficiently ambiguous that high-resolution targeting is not warranted—as many as 80-90% of candidates rated '3' will probably not show cave-like characteristics at high resolution. Many '3' candidates are classified as small rimless pits (srp, above); HiRISE imagery shows that some srp's contain structures consistent with cave entrances, but most do not. A rating of '0' indicates 'zero priority' because at least one HiRISE observation of the target already exists and is publically available as of 03/2017.

C-6. APC Diameter (Characters 34-36) – Diameter of the APC rounded to the nearest 5 meters (due to measurement uncertainties and non-perfect circular shapes). For the small number of pits with elliptical shapes, this value represents the pit's major axis. Most candidates in this catalog were identified during a survey for APC candidates; measuring non-APC candidates was outside the scope of budgeted criteria for the cave-detection survey.

C-7. APC Depth (Characters 38-40) - Approximate value calculated from shadow measurements: Generally: D=((Shadow-length) ÷ tan(incidence angle)). The observed emission angle becomes important in depth calculations when its value exceeds ~5°; in such cases, we use an elaboration of the above formula that incorporates emission-angle values (See *Cushing et al*., 2015 for the full mathematical description.). When candidates are covered by multiple observations, we typically chose that with the smallest observed incidence angle for depth calculations. Note – an APC described as 'deep' in the comment section signifies that no sunlit floor can be seen, and that only a minimum depth can be calculated. Deep APCs typically have a d/D ratio >1, which is unusual for pits throughout the solar system. Figure 2 (bottom) shows a deep APC.

C-8. Comments (Characters 42-110) – Simple details describing each candidate.

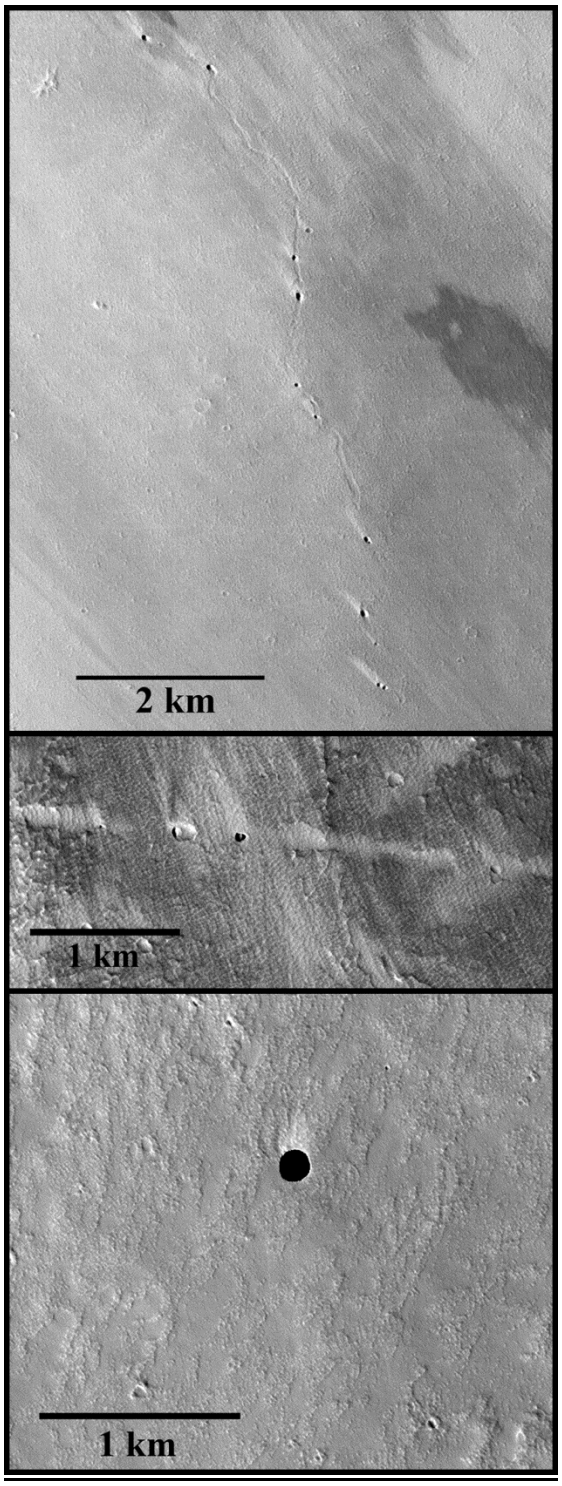


Figure 2. Three different cave entrance candidate types on Mars. Top image shows an inflated tube-fed lava flow with multiple skylight entrances (CTX: P17_007774_1757); the center image is a volcano-tectonic fracture with a skylight entrance (HiRISE: ESP_014380_1775);lower image shows an Atypical Pit Crater (APC) with a diameter of 165 m, a depth >245 m, and an overhanging rim of unknown extent (HiRISE: PSP_003647_1745 – see *Cushing*, 2012).

Additional notes on the MGC^3 dataset

1. It is important to note that all locations listed in this dataset are only *candidate* cave entrances. We can only see for a short distance beneath cave-entrance overhangs, and require additional (oblique orbital [e.g., *Robinson et al*., 2012] or in situ) observations before we can determine if any of these voids extend for substantial distances beneath the surface. Additionally, as many as 20% of the top priority targets listed here will likely fail as candidates once scrutinized by HiRISE; deeply shadowed collapse pits and other depressions are sometimes indistinguishable from open cave entrances at CTX image scales (~6 m/pixel).

2. This catalog will be updated when warranted by the accumulation of new data. Updates will include any newly identified candidates and any measurement improvements or classification changes. Failed candidates will be labeled and will remain in the dataset.

3. The CTX and HiRISE image datasets are not geodetically controlled to the martian surface and coordinates given in this catalog are approximate. Although point coordinates may display up to several hundred meters from the feature being described, there should be no ambiguity because no other cave-like features will be found nearby; each point is clearly associated with its corresponding surface feature.

4. Most of the APC data in this catalog was previously published as on-line supplementary information to [*Cushing et al*., 2015]. Updated APC measurements from subsequent HiRISE observations have been applied, this release supersedes all previously published APC data.

5. Contributions to the MGC^3 dataset are encouraged. Pease send all pertinent information (e.g., coordinates, images, etc.) to gcushing@usgs.gov. Contributions will be evaluated immediately. Accepted contributions will be included with the next data release, and the submitting person or organization will be acknowledged in the 'Comments' column.

6. *Graphical representation and shape-file conversion*: To view and use MGC^3 graphically, there is a .csv version of this catalog (in the '/miscellaneous' directory) which can be opened as a custom shape layer in the JMARS planetary GIS tool (*Christensen et al.*, 2009; free download at http://jmars.asu.edu). The authors highly recommend JMARS to view this dataset because directly accesses the HiRISE and CTX datasets, is free to the public, and offers a large selection of easy-to-use viewing and measuring tools. JMARS can also save this catalog as ESRI-formatted shape files, which can be read by other GIS software such as ArcGIS. ESRI formatted shape files are not included with this release because they are not compliant with PDS4 archiving standards. This catalog will be submitted to the JMARS team for possible inclusion as a permanent layer.

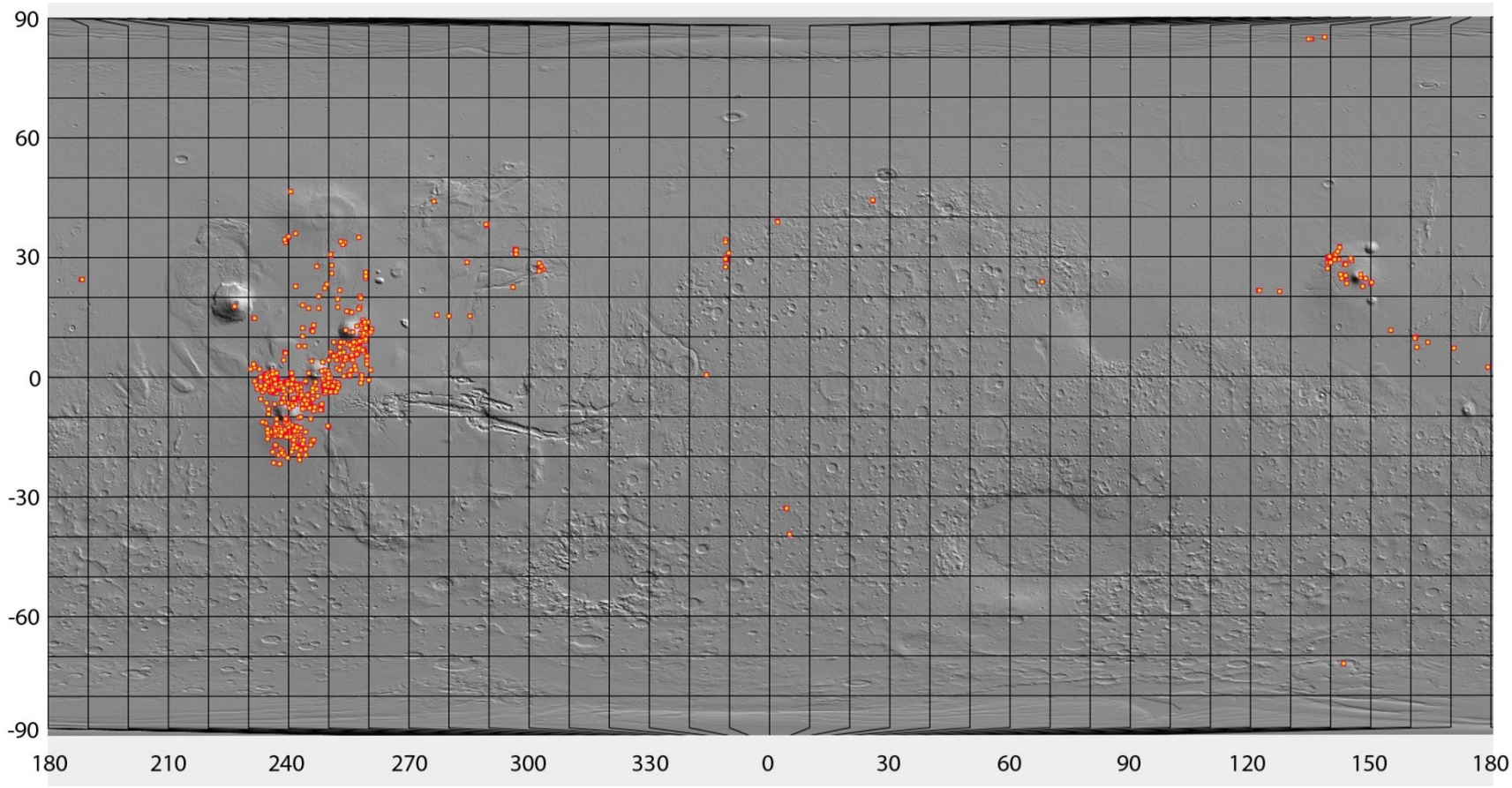


Figure 3. Global context image of currently identified martian cave-entrance candidates (1035 total). Surveys of large volcanic regions on Mars have revealed that the Tharsis region contains the greatest density of candidates identified thus far. Most of Mars' surface has yet to be surveyed for cave entrances, and the next surveys will likely concentrate on periglacial terrains and surfaces with evidence of fluvial activity along the crustal dichotomy.

4. Archive Structure

The MGC^3 archive uses the PDS4 archiving standard (*PDS4 Concepts*, 2015; *PDS4 Standards Reference*, 2015) for the archive structure and product labels. In PDS4 every object in the archive is a product, meaning that it has a detached PDS4 label expressed in XML and an associated data object.

All PDS4 products are uniquely identified by a combination of a logical identifier (LID) and a version identifier (VID). The LID and VID are separate attributes in a PDS4 label. However, they can be combined together into a versioned identifier (LIDVID) to uniquely identify and locate a particular version of a particular product throughout the entire PDS inventory. The LID for MGC^3 has the form of:

urn:nasa:pds::: <bundle_id>:<collection_id>:<product_id>

where:

urn:nasa:pds notes that this is a PDS4 product
<bundle_id> is taken from the bundle LID
<collection_id> is taken from the collection LID
<product_id> is a string to uniquely identify the product within its collection.

The LID for this version of MGC^3 is:

urn:nasa:pds:mars_cave_catalog:data:mgc3_data_v1r0

where:

mars_cave_catalolg is the bundle_id
data is the collection_id
mgc3_data is the product_id
v1r0 is the version identifier and has the form vMrn where M and n are integers. The first version of a product has a VID of v1r0. Minor changes to the product or its label cause the n to increment and major changes, such as reformatting, cause the M to increment.

mgc3_data_v1r0 is the table file name (current version) without its extension.

The product PDS4 label file has the same name but with XML for the file extension.

Acknowledgements: We are grateful to the HiRISE team for their efforts at targeting such a large number of cave-entrance candidates – many more than anticipated.

5. References

Christensen, P. R., et al. (2009), JMARS – A Planetary GIS. Available at: http://adsabs.harvard.edu/abs/2009AGUFMIN22A..06C.

Cushing, G. E., T. N. Titus, J. J. Wynne, and P. R. Christensen (2007), THEMIS observes possible cave skylights on Mars, *Geophys. Res. Lett*., 34, L17201, doi:10.1029/2007GL030709.

Cushing, G. E. (2012), Candidate cave entrances on Mars, *J. Cave Karst Stud*., 74(1), 33–47.

Cushing, G. E., C. H. Okubo, and T. N. Titus (2015), Atypical pit craters on Mars: New insights from THEMIS, CTX, and HiRISE observations, *J. Geophys. Res. Planets*, 120, 1023–1043, doi:10.1002/2014JE004735.

Gaddis, L. R., et al. (1997), An overview of the integrated software for imaging spectrometers, *LPSC XXVIII*, pp. 387–388.

Malin, M. C., et al. (2007), Context Camera Investigation on board the Mars Reconnaissance Orbiter, *J. Geophys. Res*., 112, E05S04, doi:10.1029/2006JE002808.

McEwen, A. S., et al. (2007), Mars Reconnaissance Orbiter's High Resolution Imaging Science Experiment (HiRISE), *J. Geophys. Res*., 112, E05S02, doi:10.1029/2005JE002605.

Okubo, C., and S. Martel (1998), Pit crater formation on Kīlauea Volcano, Hawai'i, *J. Volcanol. Geotherm. Res*., 86, 1–18.

Planetary Data System, Standards Reference, Version 1.4.0 (2015). Available at: https://pds.nasa.gov/pds4/doc/sr/current/StdRef_1.4.0_150922.pdf

Planetary Data System, PDS4 concepts, Version 1.4.0 (2015). Available at: https://pds.nasa.gov/pds4/doc/concepts/Concepts_150909.pdf

Robinson M. S., J. W. Ashley, A. K. Boyd, R. V. Wagner, E. J. Speyerer, B. R. Hawke, H. Hiesinger, C. H. van der Bogert (2012), Confirmation of sublunarean voids and thin layering in mare deposits, Planet. Space Sci., 69, pp. 18-27; doi:10.1016/j.pss.2012.05.008

Torson, J. M., and K. J. Becker (1997), ISIS—A Software Architecture for Processing Planetary Images, *Proc. Lunar Planet. Sci. Conf*. 28th, pp. 1443–1444.